

BMSSM Higgses at 125 GeV

F. Boudjema and G. Drieu La Rochelle

LAPTh[†], Univ. de Savoie, CNRS, B.P.110, Annecy-le-Vieux F-74941, France

October 31, 2018

Abstract

The BMSSM framework is an effective theory approach that encapsulates a variety of extensions beyond the MSSM with which it shares the same field content. The lightest Higgs mass can be much heavier than in the MSSM without creating a tension with naturalness or requiring superheavy stops. The phenomenology of the Higgs sector is at the same time much richer. We critically review the properties of a Higgs with mass around 125 GeV in this model. In particular, we investigate how the rates in the important inclusive 2γ channel, the $2\gamma + 2$ jets and the $ZZ \rightarrow 4l$ (and/or WW) can be enhanced or reduced compared to the standard model and what kind of correlations between these rates are possible. We consider both a vanilla model where stops have moderate masses and do not mix and a model with large mixing and a light stop. We show that in both cases there are scenarios that lead to enhancements in these rates at a mass of 125 GeV corresponding either to the lightest Higgs or the heaviest CP-even Higgs of the model. In all of these scenarios we study the prospects of finding other signatures either of the 125 GeV Higgs or those of the heavier Higgses. In most cases the $\bar{\tau}\tau$ channels are the most promising. Exclusion limits from the recent LHC Higgs searches are folded in our analyses while the tantalising hints for a Higgs signal at 125 GeV are used as an example of how to constrain the BMSSM and/or direct future searches.

LAPTh-013/12

[†]UMR 5108 du CNRS, associée à l'Université de Savoie.

1 Introduction

The latest upturn in the hunt for the Standard Model Higgs came at the very end of 2011, when the ATLAS and CMS collaborations both presented their analyses with the latest dataset (see [1, 2]) and showed that, besides an exclusion limit that is driving the Higgs mass in a very thin region 115-131 GeV, there might be the possibility of a Higgs signal around $m_h = 125$ GeV. If these results are confirmed they will mark the crowning of the Standard Model especially that this mass range is in excellent agreement with the indirect limit from the global electroweak precision measurements that test the inner working of the model, shall we say the theory now, at the quantum and renormalisable level.

With the fact that no new particle outside the SM has been discovered, a lone elementary Higgs may bring back the issue of naturalness. A known solution to this problem is supersymmetry. No wonder that the first flurry of articles after the announcement of a hint of a Higgs with mass around 125 GeV were from aficionados of supersymmetry. 125 GeV is an almost lucky strike for its minimal manifestation, the MSSM. Almost lucky, because in the MSSM this value is on the heavy side, requiring large values for the mass scale in the stop sector[3, 4, 5, 6, 7, 8, 9, 10]. This large scale brings back again the naturalness problem. Extended models of supersymmetry[11, 12] fare better from this point of view, in particular one of the simplest versions, namely the next-to-minimal version, the NMSSM[13, 14, 15, 7], can quite naturally provide a Higgs with $m_h = 125$ GeV. These more natural extended models allow also a richer phenomenology in the Higgs sector than in the MSSM. For example, scrutinising the data suggests that the signal corresponds to larger production rates than in the SM in the 2γ channel. This is extremely difficult to attain in the MSSM [5, 7] where apart from the large values for the scales in the stop sector to obtain the Higgs mass, one needs the collaboration of staus with the mass of the lightest stau as low as what is permitted by LEP but otherwise very large parameters for other scales in this sector also[5]. There is more flexibility with the NMSSM[13, 7, 16] when an increase in the diphoton rate comes easily as the consequence of a drop in the coupling of the Higgs to bottom quarks due to mixing with the singlet component. Although we must stress that, considering the significance of the results in the different channels and the two experiments, one should take great care in drawing any hasty conclusion, it must nonetheless be admitted that the hint of a signal is at the moment still compatible with a SM interpretation.

One could attempt to better fit the data within the most general effective Lagrangian describing the Higgs interactions within an extension of the SM[17, 18, 19]. Fits to the anomalous Higgs couplings could then be performed. This could be useful in constraining some underlying models but this approach may not be as constraining when the underlying model tightly relates the different anomalous couplings of the 125 GeV Higgs that may also have a bearing on other (heavier or lighter) Higgses that should be included in the picture. A case in mind is the Higgs sector of the BMSSM[20, 21, 22, 23, 24, 25] which is a general effective Lagrangian approach to the MSSM first introduced to address the naturalness problem[26, 27]. Masses up to 250 GeV can be naturally achieved for the lightest Higgs of the model[28, 29, 30, 31, 32, 33]. Most recent analyses of the model taking into account ATLAS and CMS data now only allow masses below 140 GeV for the lightest Higgs[32, 33]. Naturally there is no problem for the model to generate lightest Higgs masses around 125 GeV. At the same time Higgses with this mass, in this model, have a rich phenomenology with properties that can differ from those of the SM and the MSSM. It is therefore very important to review the signatures of the different manifestations of these Higgses. In particular it is crucial to see which channels, in particular the most sensitive ones: $\gamma\gamma$, $ZZ(4l)$, $\gamma\gamma + 2$ jets, in this mass range see their rates either enhanced or reduced and study correlations between these rates. This is the main purpose of this paper.

Apart from the profile of the Higgs with $m_h = 125$ GeV in terms of a signal in different channels, we take different constraints in particular non observation of signals of other Higgses with the present LHC luminosity. We then take as an example a situation where an enhancement in the inclusive diphoton channel and the $ZZ \rightarrow 4l$ is confirmed and investigate what consequences on other signals either of the same Higgs in other channels or other heavier Higgses are to be expected when more data is collected. We also review the role that the stop sector can play in the BMSSM. In these models light stops can very easily give $m_h = 125$ GeV, however very light stops with large mixings can change in an important way the correlations between the $\gamma\gamma$, $ZZ(4l)$, $\gamma\gamma + 2$ jets channels. We also investigate whether the 125 GeV Higgs could correspond to the heaviest CP even Higgs. The article is organised as follows. In section 2 we briefly describe the BMSSM set up and the main characteristics of the Higgs that ensue, and we define the parameter space and how the experimental data is incorporated. In section 3, we consider the case where the lightest CP-even Higgs, h , has mass $m_h = 125$ GeV. In section 4 we turn to a scenario where it is the heaviest Higgs, H , that has mass $m_H = 125$ GeV. Section 5 collects our conclusions.

2 BMSSM description

The BMSSM is an effective theory that builds upon the MSSM by the addition of higher order operators. This means that it shares the same field content as the MSSM, in particular in the Higgs sector the physical states are the 2 CP-even Higgses (the lightest h and heaviest H), the CP-odd A^0 and the charged Higgs H^\pm . The higher order operators represent the effect of physics beyond the MSSM that has been integrated out and is characterised by a mass scale M . The effective theory is then an expansion in powers of $1/M$ of the Kähler potential K and the superpotential W . An exhaustive set of leading order operators has been catalogued in [34] but what concerns us here are those operators that have most impact, namely those that involve the Higgs sector. Indeed, it is well known that the Higgs sector of the MSSM is very much constrained and it is thanks to the radiative corrections that the MSSM has survived so far. Likewise perturbing a little through the introduction of these higher operators changes the phenomenology of the MSSM quite drastically and improves the naturalness argument. The set of leading order operators, beyond the MSSM, is quite restricted[20, 21, 22, 23, 24]

$$W_{\text{eff}} = \zeta_1 \frac{1}{M} (H_1 \cdot H_2)^2, \quad (1)$$

$$K_{\text{eff}} = a_1 \frac{1}{M^2} \left(H_1^\dagger e^{V_1} H_1 \right)^2 + a_2 \frac{1}{M^2} \left(H_2^\dagger e^{V_2} H_2 \right)^2 + a_3 \frac{1}{M^2} \left(H_1^\dagger e^{V_1} H_1 \right) \left(H_2^\dagger e^{V_2} H_2 \right) \\ + a_4 \frac{1}{M^2} (H_1 \cdot H_2) \left(H_1^\dagger \cdot H_2^\dagger \right) + \frac{1}{M^2} \left(a_5 H_1^\dagger e^{V_1} H_1 + a_6 H_2^\dagger e^{V_2} H_2 \right) \left(H_1 \cdot H_2 + H_1^\dagger \cdot H_2^\dagger \right). \quad (2)$$

where H_1, H_2 are the two Higgs superfields in the gauge basis, assuming the hypercharges to be $Y_1 = -1, Y_2 = 1$. The new parameters ζ_1, a_i ($i = 1..6$) are the remnant of the New Physics. In order to account for supersymmetry breaking of these extra operators the simplest way is to convert those effective coefficients into spurions (see [29]) :

$$\zeta_1 \longrightarrow \zeta_{10} + \zeta_{11} m_s \theta^2, \quad (3)$$

$$a_i \longrightarrow a_{i0} + a_{i1} m_s \theta^2 + a_{i1}^* m_s \bar{\theta}^2 + a_{i2} m_s^2 \bar{\theta}^2 \theta^2. \quad (4)$$

We have introduced the spurion breaking mass m_s as a book-keeping quantity so that all effective coefficients are dimensionless. One finds that the leading corrections are of order m_s/M and

μ/M , where μ is the usual supersymmetric Higgs mixing parameter. At order $1/M^2$ corrections are of order $(m_s/M)^2$, $(\mu/M)^2$ and $(\mu m_s/M^2)$. There are also corrections of order v^2/M^2 , v is the Standard Model vacuum expectation value. We assume the underlying theory to be approximately supersymmetric so that m_s/M is small and the effective expansion well behaved. In our analysis we take

$$\frac{m_s}{M} = \frac{\mu}{M} = 0.2, \quad M = 1.5\text{TeV}. \quad (5)$$

Note that μ is (naturally) small, $\mu = m_s = 300$ GeV.

We refer the reader to references [20, 28, 29, 33] for the full derivations of the Higgs masses and couplings, in particular how the cross sections and branching fractions, either tree-level or loop induced, are computed[33]. Here we will just outline the main features.

With the coefficients (ζ, a) in the range $-1, 1$, masses for the lightest Higgs up to 250 GeV can be obtained. The largest values are obtained for the smallest t_β in the range $2-40$. t_β is the ratio of the vacuum expectation values of the Higgs doublets. The coupling VVh/H ($V = W^\pm, Z$) can not be larger than 1 but can be very much reduced. The implementation imposes a custodial symmetry, then the WWh and ZZh are to a very good approximation equal. $t\bar{t}h$ is not much affected especially compared to $b\bar{b}h$ that can be either greatly reduced or enhanced. This has important consequences for gluon fusion and the branching fraction of the Higgs into photons and ZZ in the range of interest around 125 GeV.

LEP, Tevatron and in particular the LHC data have put dramatic constraints on the model[33]. Taking into account the status of the searches at ATLAS and CMS with a dataset up to 2.3 fb^{-1} [35] (the parameter space and the experimental constraint being discussed in the following part), the lightest higgs, h can not be heavier than 140 GeV, see fig. 1. Note that the data allow for the heaviest CP even Higgs, H , to be quite light with $m_H = 125$ GeV, with a light Higgs, h , escaping the LEP bounds. There is therefore the possibility that the the hint for an excess at 125 GeV may be due to H with h being more elusive, a possibility that we will address.

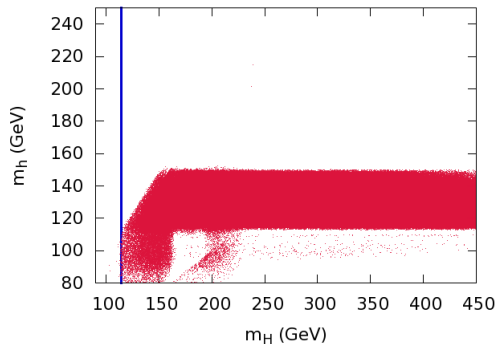


Figure 1: We plot here the allowed region in the m_H, m_h plane with the 2 fb^{-1} dataset from LHC. For more details, see [33].

The production channels are also modified. Gluon fusion ($gg \rightarrow h$) can be either greatly enhanced or suppressed : when normalized to the SM expectation its value ranges from 0.1

to higher than 5. Vector boson fusion, $VV \rightarrow h/H$, on the other hand can only be reduced. The b fusion ($b\bar{b} \rightarrow h$) can be greatly enhanced or reduced with respect to the SM prediction. It is important to note that the production mechanisms that contribute to the same inclusive channel are not rescaled in the same way : hence the differential distributions of the BMSSM Higgs production will not be exactly the same as the SM ones since each production mode can lead to different kinematic properties. This remark should be kept in mind when exploiting SM limits based on inclusive cross section. We discussed this issue at some length and gave recommendations in[33].

For the decays of the Higgses, the branching ratios can also be enhanced or suppressed, however these changes are not independent from how the production rates are affected. Since we are interested in the mass range around $m_h = 125$ GeV, we plot in figure 2 the normalised value of the gluon fusion as a function of the normalised branching ratio into photons for h , with red (blue) points for $R_{\gamma\gamma} < 1$ ($R_{\gamma\gamma} > 1$) in the range $122 < m_h < 128$ (GeV). In this scenario the stop sector has little impact. The ratio $R_{\gamma\gamma}$, to be better specified later, corresponds to a good approximation to the product of the normalised gluon fusion and normalised branching ratio into photons. As can be seen, enhancing the branching ratio into photons has a strong consequence on gluon fusion. An enhanced branching fraction into photons forces $\sigma_{gg \rightarrow h}$ to have an almost SM rate. For the highest value of $Br(h \rightarrow \gamma\gamma)/Br^{SM}(h \rightarrow \gamma\gamma)$, $\sigma_{gg \rightarrow h}/\sigma_{gg \rightarrow h}^{SM} \sim 1.2$. This slight increase , together with the structure of the correlation (the two branches) see fig. 2,

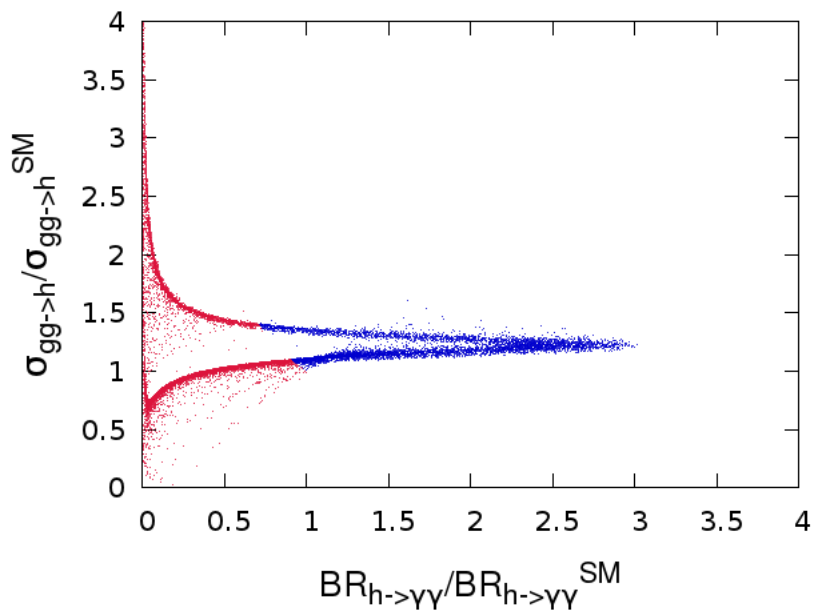


Figure 2: We show here the gluon fusion normalised to the SM expectation as a function of the normalised branching ratio to photons in the BMSSM, with $122 < m_h < 128$ (GeV), before applying collider constraints. The effect of the stops is negligible here.

can be understood as follows. In this set-up $gg \rightarrow h$ is driven mostly by the top contribution that is practically standard model like and the bottom contribution that can vary greatly. In the SM, the small b contribution interferes destructively with the dominant top contribution. If

now we parameterise the strength of the $h\bar{b}b$ in the BMSSM as $h^{\text{BMSSM}}\bar{b}b = x_b h^{\text{SM}}\bar{b}b$, then we approximately have

$$\frac{\sigma_{gg\rightarrow h}}{\sigma_{gg\rightarrow h}^{\text{SM}}} = \frac{(1 - \epsilon_{bt}x_b)^2}{(1 - \epsilon_{bt})^2} \quad 0 < \epsilon_{bt} \ll 1, \quad (6)$$

ϵ_{bt} is the relative contribution of the bottom compared to the top, at the amplitude level. Largest values of $Br(h \rightarrow \gamma\gamma)/Br^{\text{SM}}(h \rightarrow \gamma\gamma)$ are due to a much reduced $h \rightarrow \bar{b}b$ width and hence small $|x_b|$. Then for $|x_b| < 1$

$$\begin{aligned} \frac{\sigma_{gg\rightarrow h}}{\sigma_{gg\rightarrow h}^{\text{SM}}} &= \frac{(1 - \epsilon_{bt}x_b)^2}{(1 - \epsilon_{bt})^2} \sim 1 + 2\epsilon_{bt}(1 - x_b) > 1, \\ &\simeq 1 + 2\epsilon_{bt} \quad x_b \rightarrow 0. \end{aligned} \quad (7)$$

which is the contribution of the bottom contribution. The bell shape is a reflection of the quadratic dependence $(1 - \epsilon_{bt}x_b)^2$. We should keep this characteristic in mind for the rest of the analysis. Therefore despite what might seem to be a relative freedom with the new parameters introduced by the BMSSM, some predictions are rather constrained. Let us add a comment about the reduction of the $h\bar{b}b$ coupling. With $m_h \sim 125$ GeV, even a relatively large reduction which is accompanied by an almost similar reduction of the $h\bar{\tau}\tau$ coupling, might still not affect so drastically the $Br(h \rightarrow \bar{b}b)$ nor the $Br(h \rightarrow \bar{\tau}\tau)$ since $\Gamma(h \rightarrow \bar{b}b)$ might still remain dominant.

2.1 The parameter space

t_β and m_{A^0} (the mass of the pseudoscalar Higgs) are varied in the following range.

$$t_\beta \in [2, 40], \quad m_{A^0} \in [50, 450].$$

Considering the impact of the third family on Higgs physics, we allow some flexibility in the stop sector. Two implementations will be considered.

- Model A: A no mixing scenario, where all soft masses of the third generation squarks are set to $M_{u3R} = M_{d3R} = M_{Q3} = 400$ GeV with no mixing, in particular the stop mixing parameter $A_t = 0$. For these values the masses $m_{\tilde{t}_1}, m_{\tilde{t}_2}$ are around 400 GeV and the mixing angle vanishes. This is taken as a standard case, where stops are not too heavy and in the set up of the BMSSM their effect is not so important.
- Model B: A maximal mixing scenario where one of the stop is light $m_{\tilde{t}_1} = 200$ GeV. We will take $m_{\tilde{t}_2} \in [300, 1000]$ (GeV) and $\sin 2\theta_{\tilde{t}} = -1$. The heaviest stop mass is taken as a free parameter. This will have important consequences in the production of the Higgses and their decays. Note that, in a generic model, a 200 GeV stop can still escape all current collider limits.

For the rest of the MSSM parameter space, the following values have been used : all soft masses are set to $M_{\text{soft}} = 1$ TeV (except for the third generation), μ and M_2 (the $SU(2)$ gaugino mass) are set to 300 GeV, M_1 (the $U(1)$ bino mass) is fixed by the universal gaugino mass relation $M_1 = \frac{5}{3} \tan^2 \theta_W M_2 \simeq M_2/2$, and $M_3 = 800$ (the $SU(3)$ gaugino mass) GeV, $\cos^2 \theta_W = M_W^2/M_Z^2$. All trilinear couplings are set to 0 (except A_t).

For the purpose of this paper this last set of parameters has practically no impact, so we could have taken lower values of M_{soft} and M_3 compared to the new scale $M = 1.5$ TeV. In

scenario B, the largest value of the heaviest stop $m_{\tilde{t}_2} = 1$ TeV that we allow in the scan should be regarded an extreme example, not only from the point of view of naturalness but also because it is not far heavier than the new scale $M = 1.5$ TeV. This said we must emphasise that most of our study is done with $m_{\tilde{t}_2} = 600$ GeV. Furthermore the heavy scale M can be enhanced with little change to our results provided one keeps fixed the ratios $m_s/M, \mu/M$.

The effective coefficients, (ζ, a) will be varied in the range $[-1, 1]$. The following constraints were applied on each point, in order to constrain the effective parameter space (see [33] for more details) :

- Perturbativity check. We check that $1/M^3$ contributions to m_h are small enough. Indeed one must make sure that the perturbative expansion in $1/M$ is under control. This means that on top of all experimental constraints that we take into account, we also check that our points exhibit a correct effective expansion by keeping only points where the third order (*i.e.* $1/M^3$ terms) contribution to the light Higgs mass is within 10% of its value.
- Electroweak Precision tests. Since the effective coefficients have a non vanishing contribution to oblique parameters, we verify the consistency with the electroweak precision measurements.
- LEP and Tevatron Higgs searches. This applies to all Higgses : h, H, A^0, H^\pm , including top decays to H^\pm .
- ATLAS and CMS Higgs searches. The list of channels that we take into account and how these are exploited within the BMSSM is detailed in [33]. As concerns the exclusion limits exploiting the $\bar{\tau}\tau$ channels we had also included in [33] the MSSM analysis of ATLAS and CMS. Concerning the mass range 122 – 128 GeV and an interpretation in terms of a signal, we detail our approach in section 2.2.

In this work we do not include constraints based on flavour physics ($((g-2)_\mu, B_s \rightarrow \mu^+\mu^-, \dots)$) and dark matter (relic density) constraints. For the former, this will introduce some extra model dependence from extra operators in the BMSSM, outside the Higgs sector. For the relic density it is known that the prediction can change drastically if we change the cosmological model. These issues may obscure the conclusions on the interpretation of the possible Higgs signal. We will certainly come back to these effects in future investigations.

2.2 Input from the LHC

In order to use the results from the ATLAS and CMS collaborations, we have used the following ratios

$$R_{XX} = \frac{\sigma_{pp \rightarrow h \rightarrow XX}}{\sigma_{pp \rightarrow h \rightarrow XX}^{SM}} \quad \text{and} \quad R_{XX}^{\text{exclusion}} = \frac{\sigma_{pp \rightarrow H \rightarrow XX}}{\sigma_{pp \rightarrow H \rightarrow XX}^{\text{excluded 95\%}}}, \quad (8)$$

where XX denotes a particular final state (say the inclusive 2γ). $\sigma^{\text{excluded 95\%}}$ stands for the 95% C.L. excluded cross-section reported by the collaborations. In practice the R_{XX} will be used in the signal case, to compare with the best fit $\hat{\mu}$ – of the so called signal strength μ – given by the experiments. In eq. 8, h in the BMSSM will refer either to the lightest or heaviest CP-even Higgs. $R_{XX}^{\text{exclusion}}$ will be used in the no-signal case as a measure of the sensitivity of the search, here H stands for all Higgses not contributing to a signal in the mass range 122 – 128 GeV. It will also be shown as a measure of the luminosity needed to see the effect of a particular Higgs in a certain channel in the future. For R_{XX} the most important channels are the inclusive 2γ , $ZZ \rightarrow 4l$ (ATLAS and CMS) and the exclusive $2\gamma + 2jets$ (CMS). For $R_{XX}^{\text{exclusion}}$ we use the full

dataset across all Higgs masses covered by the experiments with the current collected luminosity of 4.9fb^{-1} . As we said $R_{XX}^{\text{exclusion}}$ gives a measure of the luminosity needed to uncover a signal in a new channel. The current $R_{XX}^{\text{exclusion}}$ is based on a collected luminosity of about 4.9fb^{-1} for the LHC running at 7 TeV. To extract from the plots for $R_{XX}^{\text{exclusion}}$ that we will show the approximate luminosity that will be needed to uncover a potential signal, one can base the rough estimate on a simple rescaling of the luminosity. For example in the plots we will show, a channel with $R_{XX}^{\text{exclusion}} = 0.1$ will require a luminosity of about 500fb^{-1} to be observed. With a luminosity of 30fb^{-1} only those channels with $R_{XX}^{\text{exclusion}} > 0.4$ may be accessible.

We decided not to carry out a fit of the model to the data (as was done in [19, 18] among others) for the reason that so far the signals from both collaborations are not so easy to reconcile and also because in view of the quality of the results this exercise is far too premature. We chose instead to focus on assessing the limits on the flexibility of the BMSSM with a Higgs in the range $122 < m_h < 128$ GeV, a range broad enough that it takes into account the hints from both experiments including the uncertainty on the mass in each experiment. We leave a complete computation of the compatibility of the model with the data for the future, hopefully more precise, set of data. By using those ratios instead of computing the complete likelihood function (as was tried in [18]), we have implicitly assumed some approximations that are discussed in [33]. In the inclusive channels, we neglect for instance the effect of acceptance and efficiency cuts due to the change in the relative contribution of the different production modes (gluon fusion, vector boson fusion and associated production, b quark fusion) compared to the Standard Model. In other words, we are taking ratios of inclusive cross-sections. For analyses that are truly inclusive, such as the $h \rightarrow ZZ \rightarrow 4l$ there is hardly any difference (see [33]), but the situation changes when channels are divided in subchannels with different final states. The $h/H \rightarrow WW + 0/1/2$ jets comes to mind. The difficulty is that each subchannel that contributes to the inclusive cross section has a different efficiency and the fact that most often the rates for the different channels in the BMSSM are not rescaled by the same factor. The reason for these approximations is that most of the experimental quantities, such as the efficiency and the acceptance for each production mode or the cross-section limits for each subchannels, are so far unavailable, forbidding hence an exact interpretation. So we reiterate our recommendation that efficiencies be provided (see the Les Houches Recommendations for the Presentation of LHC results [36] for a detailed discussion on the subject.). However, for the time being those approximations do not prevent a qualitative survey of the would be Higgs signal properties.

Having said that, CMS[37] has most recently provided data for a more exclusive observable, $2\gamma + 2\text{jets}$. The latter is more sensitive to the production through vector boson fusion, with the Higgs subsequently decaying into 2 photons. We take this observable into account. The contribution of the $gg \rightarrow h$ to this channel is however not negligible. Fortunately the CMS collaboration[37] does provide the overall acceptance/efficiency (product of the two) for each of the important channels (this applies also for the BMSSM), albeit for a single Higgs mass, $m_h = 120$ GeV. The overall acceptance is quoted as 0.15 for production through Vector Boson Fusion (VBF) and 0.005 for gluon fusion. We therefore simulate the ratio $R_{\gamma\gamma+2\text{jets}}$ as

$$R_{\gamma\gamma+2\text{jets}} = \frac{0.15 \sigma_{\text{VBF}} + 0.005 \sigma_{gg \rightarrow h}}{0.15 \sigma_{\text{VBF}}^{\text{SM}} + 0.005 \sigma_{gg \rightarrow h}^{\text{SM}}} \times \frac{BR_{\gamma\gamma}}{BR_{\gamma\gamma}^{\text{SM}}} \quad (9)$$

We checked that this parametrisation of $\sigma_{\gamma\gamma+2\text{jets}}$ when folded in with the SM cross sections for the LHC at 7 TeV[38] and taking into account the luminosity quoted by CMS reproduced quite exactly the number of selected events given by CMS [37]. We assume that this parametrisation that was verified to be excellent for $m_h = 120$ GeV still holds to a very good degree in the range $122 < m_h < 128$ GeV.

In order to determine if a Higgs is excluded, we use a quadrature combination of all $R^{\text{exclusion}}$

from all channels of both experiments and checked if the result was below 1. We apply the test on all Higgses (h, H, A^0, H^+), adding ratios when the Higgs bosons are degenerate, before determining whether the parameter point is allowed.

The signal condition we will require is the following : first we require a Higgs (heavy or light) boson in the range 122 – 128 GeV. Then, we discard any exclusion limit on this Higgs in the $\gamma\gamma$, ZZ and WW channels (since we want it to be a signal in those channels). We apply on all other channels and on all other Higgses the latest exclusion limits, obtained with the 4.9 fb^{-1} dataset.

2.3 Signal features, data

The data that is most indicative of a possible signal is the following (uncertainties correspond to the 1σ band)

★ ATLAS[39]:

The ATLAS collaboration records a combined (all channels) signal strength of $1.5^{+0.6}_{-0.5}$ at $m_h = 126 \text{ GeV}$. It may be considered as most revealing in channels with best resolutions on the Higgs mass:

- The inclusive $\gamma\gamma$ channel where the signal strength is $2^{+0.9}_{-0.8}$
- $ZZ \rightarrow 4l$ channel where the signal strengths is $1.2^{+1.2}_{-0.8}$ compatible with $WW \rightarrow ll\nu\nu$, though the WW channel has a worse mass resolution.

★ CMS collaboration[2] reports a combined signal strength of $1.2^{+0.3}_{-0.4}$ at $m_h = 124 \text{ GeV}$

- In the $\gamma\gamma$ channels, the first CMS release with 4.9 fb^{-1} was based on an analysis with four subchannels that gave a signal strength of 1.7 ± 0.8 at $m_h = 123.5 \text{ GeV}$ (see ref ([40])). The updated release added a dijet-tagged subchannel $\gamma\gamma + 2 \text{ jets}$ yielding by itself a signal strength of $3.8^{+2.4}_{-1.8}$. The combination of the five subchannels yield a signal strength of $2.1^{+0.8}_{-0.7}$ ([37]).
- For the $ZZ \rightarrow 4l$, $0.5^{+1.0}_{-0.7}$. Note that the mean is low, moreover the mean value for m_h is at 126 GeV.
- the $b\bar{b}$ and $\tau^+\tau^-$ channels analysed by CMS[40] in the mass range 122 – 128 GeV have so much uncertainty that they are of little use in the present analysis.

Let us take breath and emphasise again that there is still much uncertainty in these results, some of which may not help in drawing a coherent picture, expect perhaps in the $\gamma\gamma$ channel. The signal strengths are compatible with a Standard Model Higgs, however it is tempting and in any case educative to entertain the idea that some non standard Higgs scenario is emerging. What is very interesting is that the different channels and subchannels will allow, when measured with better precision, to discriminate between different models and implementations of the BMSSM. Most probably a first step in this discrimination in this mass range will be performed with $\gamma\gamma, VV, \gamma\gamma + 2\text{jets}$ perhaps also with the incorporation of the $\bar{\tau}\tau$ channel. In the case of a multi-Higgs system this will be done in parallel with searches for other Higgses. In the rest of the paper we will investigate what kind of correlations between these observables are possible within the BMSSM, for example whether enhancements in all channels are possible.

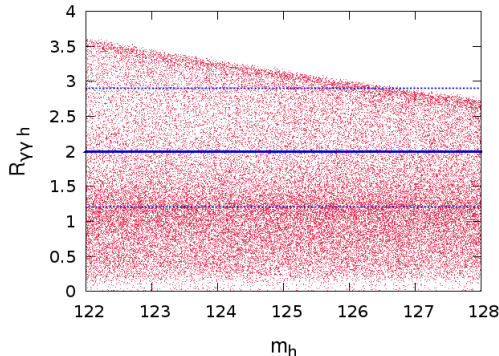


Figure 3: Allowed region in the plane $m_h, R_{\gamma\gamma}$. The blue line represents the ATLAS best fit for the signal strength, and the dotted lines are the one sigma deviations from this value in model A.

3 h as a signal in the 122 – 128 GeV window

3.1 Model A: No light stops, no mixing in the stop sector

Fig. 3 shows that with the current data, the BMSSM yields a production rate in the inclusive $pp \rightarrow h \rightarrow \gamma\gamma$ that can be quite small (as small as 0.1), and hence unobservable with the current luminosity or in the very near future. More interestingly there is however no difficulty finding a signal in this channel that is up to 3.5 times that of the SM. There is a very strong correlation with the signatures in the other promising channels: $VV \equiv ZZ \rightarrow 4l$ and the $2\gamma + 2 \text{ jets}$, see fig 4. With small differences we have $R_{\gamma\gamma} \simeq R_{ZZ} \sim R_{\gamma\gamma+2 \text{ jets}}$. Rates above those of the SM are mostly driven by reduction in the width of to $b\bar{b}$ which increases all channels. This is trivially seen for the 2γ versus ZZ channel. In the case of the $\gamma\gamma/\gamma\gamma + 2 \text{ jets}$ correlation, when the rates are above those of the SM, the inclusive channel is higher by 20% or so, this (and the appearance of two branches) rests on the same argument that we put forth in section 2 about the contribution of the b quarks. Therefore a configuration with $R_{ZZ \rightarrow 4l} = 1, R_{\gamma\gamma} = 2, R_{\gamma\gamma + 2 \text{ jets}} = 3$ is very much disfavoured in Model A.

It is important to stress that the characteristics we find in these scenarios occur for all values t_β , even if statistically, with a simple scan, the population with smaller t_β is larger.

3.2 Model B: a light stop with large mixing in the stop sector

It has been known for some time[41, 42] that, within the MSSM, light stops endowed with a large mixing can drastically reduce the gg induced production. Even if this is accompanied by an increase in the decay width to photons, the combined effect can be a large drop in $gg \rightarrow h \rightarrow \gamma\gamma$. This effect is encapsulated in the coupling of the stops to the Higgs. The coupling of the lightest stop, \tilde{t}_1 , $g_{h\tilde{t}_1\tilde{t}_1}$ writes in the large m_{A^0} limit

$$g_{h\tilde{t}_1\tilde{t}_1} \simeq \frac{g}{M_W} \left(\sin^2(2\theta_{\tilde{t}}) \frac{m_{\tilde{t}_1}^2 - m_{\tilde{t}_2}^2}{4} + m_{\tilde{t}}^2 + O(M_Z^2) \right) \quad (10)$$

$\theta_{\tilde{t}}$ is the mixing angle of the stops. The \tilde{t}_2 coupling is obtained through $\tilde{t}_1 \leftrightarrow \tilde{t}_2$. The non mixing term $m_{\tilde{t}}^2$ adds up with the top contribution, whereas the mixing term interferes *destructively*

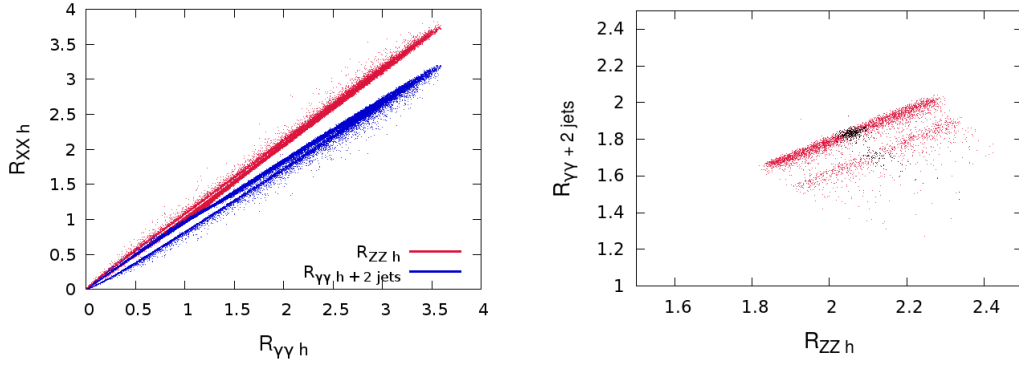


Figure 4: *Left panel: correlation between $R_{\gamma\gamma}$, R_{ZZ} and $R_{\gamma\gamma+2 jets}$ for $122 < m_h < 128$ GeV. Right panel: Imposing $R_{\gamma\gamma h} = 2.0 \pm 10\%$ (points in red) and $R_{\gamma\gamma h} = 2.0 \pm 1\%$ (points in black) we show the correlation in the plane R_{ZZ} and $R_{\gamma\gamma+2 jets}$. Both figures are for model A.*

with the top. For large mixing with large enough gap between the two stops masses this means that a reduction in $gg \rightarrow h$ occurs but accompanied with a more modest increase in the $h \rightarrow \gamma\gamma$ due to the W loop. Of course the $Br(h \rightarrow \gamma\gamma)$ can be much more efficiently increased if a drop in $h \rightarrow b\bar{b}$ occurs as within the BMSSM. Therefore we see that by letting light stops jump into the game and keeping a ratio in the $\gamma\gamma$ channel higher than the standard model, the correlations between the different channels will change.

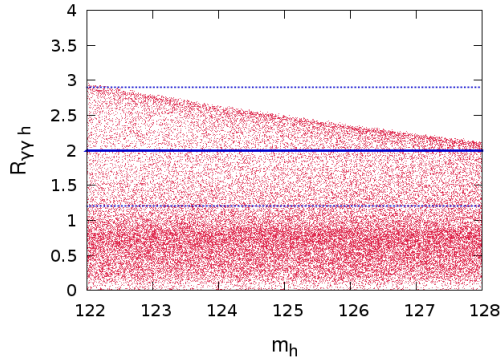


Figure 5: *Allowed region in the plane $m_h, R_{\gamma\gamma}$. The blue line represents the ATLAS best fit for the signal strength, and the dotted lines are the one sigma deviations from this value in model B with maximal mixing and with $m_{\tilde{t}_2} = 600$ GeV.*

We first note, see fig. 5, that in the maximal mixing case $\sin^2(2\theta_{\tilde{t}}) = 1$ and with $m_{\tilde{t}_2} = 600$ GeV, $R_{\gamma\gamma}$ is reduced somehow compared to the non mixing case of model A, however one still obtains enhancements of a factor 2 (and more) compared to the SM. However, now the $\gamma\gamma+2 jets$ can be much higher than the $\gamma\gamma$ channel, whereas previously we had $R_{\gamma\gamma+2 jets} = 1.5$ for $R_{\gamma\gamma} = 2$, now for the same value of $R_{\gamma\gamma}$ $R_{\gamma\gamma+2 jets} = 2.5$, see fig. 6. Moreover the weight between $R_{\gamma\gamma+2 jets}$ and R_{ZZ} has been inverted, we now have $R_{\gamma\gamma+2 jets} > R_{ZZ}$. Scanning over $m_{\tilde{t}_2}$ from 300 GeV

to 1 TeV will open up more possibilities for the correlations between these channels. The results of this scan are shown in the right panel of fig. 6. For example imposing that $R_{\gamma\gamma} = 2.0 \pm 10\%$ one can obtain $R_{\gamma\gamma + 2 \text{ jets}} = 3.8$ together with $R_{ZZ} = 1.3$. We can therefore recover values that correspond to the best fits for these observables obtained by the two collaborations. We stress again that this is illustrative and shows how much flexibility in the model can be introduced. While in the case of no-mixing in the stop sector all channels seemed to have nearly trivial correlations, raising the mixing will in most cases raise the $\gamma\gamma + 2 \text{ jets}$ channel compared to the $\gamma\gamma$ channel, and also decrease the $ZZ \rightarrow 4l$ channel with respect to the $\gamma\gamma$ one.

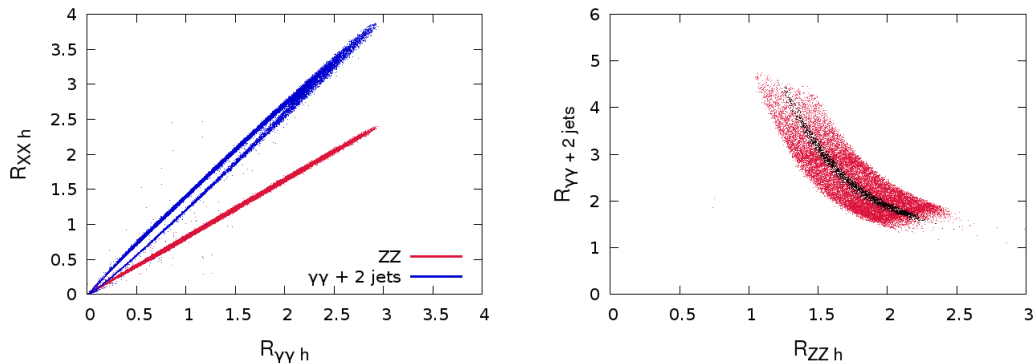


Figure 6: *Left panel: correlations between $R_{\gamma\gamma}$, R_{ZZ} and $R_{\gamma\gamma+2 \text{ jets}}$ for $122 < m_h < 128 \text{ GeV}$ in the maximal mixing scenario of model B with $m_{\tilde{t}_2} = 600 \text{ GeV}$. Right panel is a subset after imposing $R_{\gamma\gamma h} = 2.0 \pm 10\%$ (points in red) and $R_{\gamma\gamma h} = 2.0 \pm 1\%$ (points in black) in the plane R_{ZZ} and $R_{\gamma\gamma+2 \text{ jets}}$ in model B scanning in the range $m_{\tilde{t}_2} \in [300, 1000] \text{ (GeV)}$*

3.3 Prospects for other signals

Although an unambiguous signal refuting the SM would be, in the case where the signal at $m_h = 125 \text{ GeV}$ were confirmed, a precise determination of the signal strength above (or below) the SM expectation, such a precision may require some time. At the same time as the luminosity increases other channels and signatures may become sensitive in corroborating the signals with $m_h \sim 125 \text{ GeV}$. These channels could either be other channels where the same Higgs with mass 125 GeV takes part or channels affecting the other Higgses of the model. In the first case, the other allowed decay modes are $\bar{\tau}\tau$ and $\bar{b}b$ final state, however if the trend towards an increase in the 2γ , ZZ and $2\gamma + 2 \text{ jets}$ is reinforced requiring a reduced $hb\bar{b}$ (and consequently $h\bar{\tau}\tau$) in the BMSSM, the $\bar{\tau}\tau$ and $\bar{b}b$ whose current sensitivity in the SM is quite low will require substantial increase in the luminosity.

To pursue this investigation about the prospects of signals in other channels, we keep for the sake of illustration those models compatible with

$$1.2 < R_{\gamma\gamma} < 2.9 \quad \& \quad 0.5 < R_{ZZ} < 2.4, \quad (11)$$

which is the one sigma band obtained by the ATLAS collaboration and show the different $R_{XX}^{\text{exclusion}}$. Again, eq. 11 is an arbitrary choice, taken for the sake of concreteness. One should keep in mind that as more data is collected, this requirement will become stronger or perhaps even totally irrelevant.

3.3.1 Non-mixing scenario

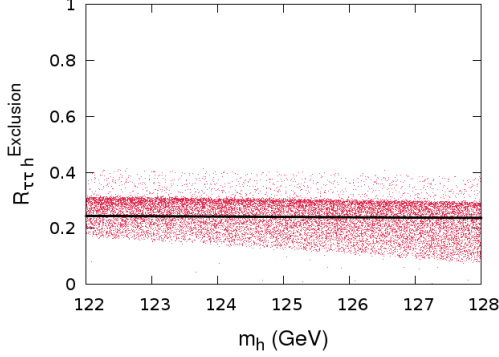


Figure 7: *Discovery perspective for the channel $h \rightarrow \bar{\tau}\tau$. The line is black corresponds to the SM.*

We start with the $\bar{\tau}\tau$ signal of h . We see in fig. 7 that $R_{h\bar{\tau}\tau}^{\text{exclusion}}$ is always below 0.4, with a concentration below 0.3 that corresponds also to the expectation from a SM Higgs, therefore a luminosity in excess of 30fb^{-1} is needed in the most favourable cases. Most cases will require much more luminosity, up to 500fb^{-1} in the worst case. Incidentally we note that this channel, despite the reduced $h\bar{\tau}\tau$ coupling, can be above that of the SM, which shows that a reduced $h\bar{\tau}\tau$ does not mean a large drop in the $\bar{\tau}\tau$ branching ratio, moreover the production cross section can be larger than in the SM.

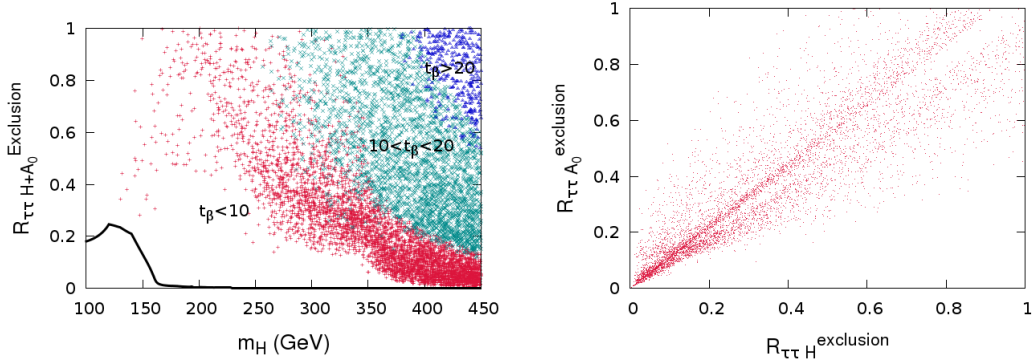


Figure 8: *Discovery perspective in the $\bar{\tau}\tau$ channel through the heavier Higgses: in the case where A^0 and H are degenerate within 10 GeV (left panel) and when A^0 and H are not degenerate (right panel). In the latter the correlations between the two signal is shown. In the panel on the left, the SM case is shown in black. The different shades for the BMSSM correspond (from left to right) to cases with $t_\beta < 10$ (red), $10 < t_\beta < 20$ (green) and $t_\beta > 20$ (blue).*

Would the other Higgses be more sensitive? The answer can be drawn from fig. 8. Some sce-

narios can be probed with little increase in the present luminosity. Generically, high t_β ($t_\beta > 20$) will be probed within the next 30 fb^{-1} , while low t_β ($t_\beta < 10$) could be quite hopeless if the heavier Higgses are heavier than 400 GeV . We find that $R^{\text{exclusion}} > 0.9$ are reached in cases where A^0 and H are close enough in mass to be degenerate ($|m_{A^0} - m_H| < 10 \text{ GeV}$), yielding thus a single signal. $R^{\text{exclusion}} > 0.9$ is reached also when the degeneracy is lifted, in which case one expects both signals to be revealed with roughly the same luminosity, see the correlation in fig. 8. Models with $m_H \sim m_{A^0} < 250 \text{ GeV}$ (degenerate case) show a ratio $R_{\tau\tau}^{\text{exclusion}} > 0.4$, which means that the region where the decoupling is not complete between light and heavy Higgses could be probed with about 30 fb^{-1} . In the non-degenerate case, there is of course a loss of a factor two, but there is still a lower limit to the exclusion ratio in this mass range. But in many models, $R^{\text{exclusion}} < 0.4$ A^0 and H will go undetected even with a luminosity in excess of 30 fb^{-1} . This discussion shows that studying the τ channel in Higgs physics is crucial. Not only it can deliver new signals but can give important information on the parameters of the model.

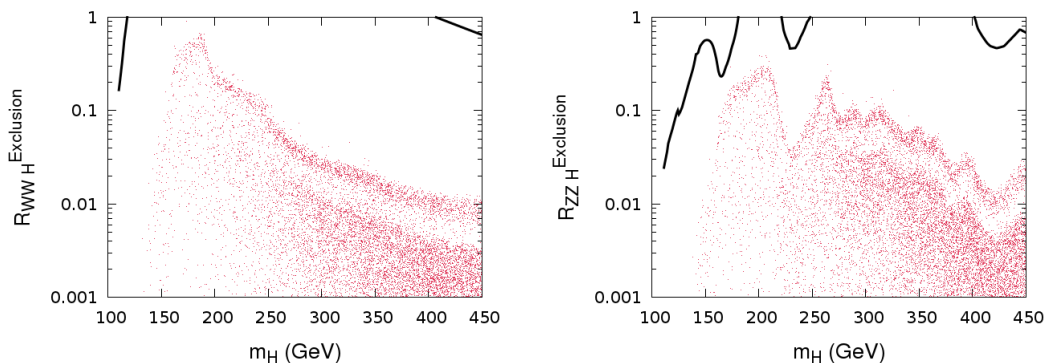


Figure 9: *Discovery perspective for other signals : $H \rightarrow ZZ$ on the left and $H \rightarrow WW$ on the right. No mixing or light stops are assumed. The curve in black is the SM Higgs hypothesis. For WW , the curve is out of the bounding box, this confirms that for Higgs masses above the WW threshold this channel is very constraining.*

Other channels offer little prospects, apart if $M_H \sim 180 \text{ GeV}$ where the search sensitivity in the clean WW and somehow also the ZZ channel is high, despite the fact that the HWW is quite small, see fig. 9.

3.3.2 Maximal mixing

In the maximal mixing case, with $m_{\tilde{t}_2} = 600 \text{ GeV}$, there are few differences. The drop in $gg \rightarrow h$ is the reason behind the drop in sensitivity. Subsequently the $\tau\tau$ channel of h will be even less sensitive, as can be seen in fig. 10. $R_{h\tau\tau}^{\text{exclusion}}$ is now below 0.2.

As concerns the heavier Higgses, the changes are marginal compared to the no-mixing case. The best prospects are in the τ channels and in the WW channel if $m_H \sim 180 \text{ GeV}$. The corresponding figures are similar to those shown for the no mixing case and we therefore do not display them here.

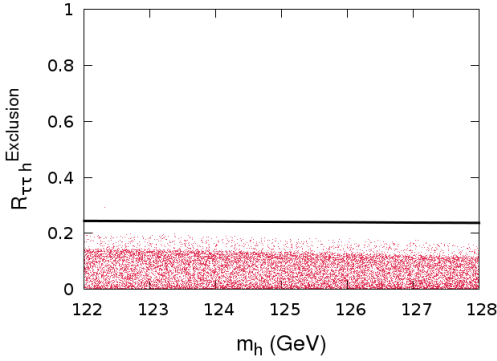


Figure 10: *Discovery perspective for the channel $h \rightarrow \bar{\tau}\tau$ in the maximal mixing scenario. The line in black represents the SM.*

4 H as a signal in the 122 – 128 GeV window

As fig. 1 makes clear, the BMSSM is compatible with a scenario where it is the heavier of the two CP even Higgses, H , which is in the range 122 – 128 GeV and may thus be responsible for a signal, while the lightest Higgs h has so far gone undetected. Such possibility, even though restrained, has also been evoked in the case of the MSSM[3]. We review such a possibility in the case of the BMSSM both in a scenario with no stop mixing and a scenario with large stop mixing and light stops.

4.1 Model A: No light stops, no mixing in the stop sector

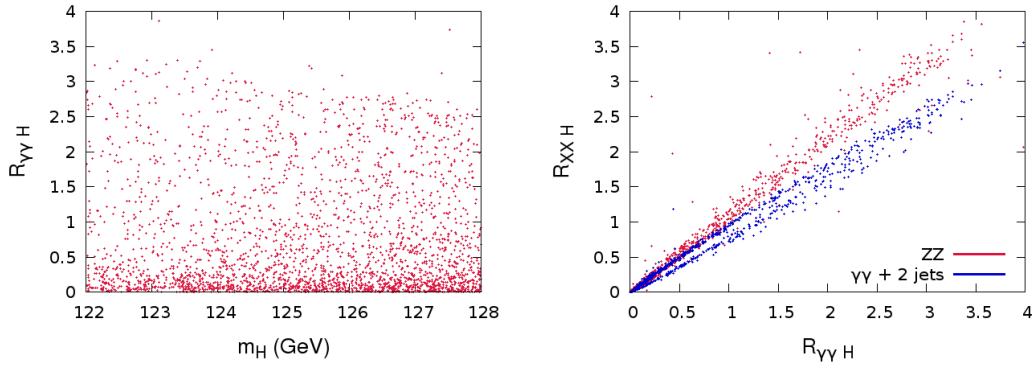


Figure 11: *We show here the allowed region in the plane $m_H, R_{\gamma\gamma}$ (left panel) and the associated correlations between $R_{\gamma\gamma}$, R_{ZZ} and $R_{\gamma\gamma+2\text{ jets}}$ for $122 < m_H < 128$ GeV (right panel) in the scenario with no-mixing .*

The statement we have just made can be made more quantitative. Solutions with $122 < m_H < 128$ GeV correspond to a situation where all three Higgses are light in the sense of being

all three below the WW threshold, $m_h < 120$ GeV $m_{A^0} < 160$ GeV. We find that some features, for the signal observables, are to a large extent similar to what we have found in the case of h . In a way the h and H have swapped their role as to which is the SM-like, SM-like as concerns the VVH/h strength. Indeed, this is illustrated in fig. 11. $R_{\gamma\gamma}$ can still reach values as large as 3.5, there are correlations between $R_{\gamma\gamma}$, R_{ZZ} and $R_{\gamma\gamma+2 \text{ jets}}$ with $R_{ZZ} > R_{\gamma\gamma+2 \text{ jets}}$ in most cases, but not all as was the case for $122 < m_h < 128$ GeV. In this case, there is some spread in the correlations between R_{ZZ} and $R_{\gamma\gamma+2 \text{ jets}}$, see fig. 11.

Let us turn to other characteristics of these BMSSM scenarios and how they could show up in other observables. Another mode where H could be observed is the $H \rightarrow \bar{\tau}\tau$ channel.

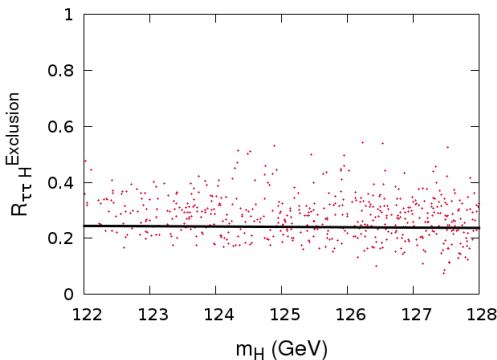


Figure 12: $R_{\tau\tau H}^{Exclusion}$ for $122 < m_H < 128$ GeV. No mixing in the stop sector is assumed. The line in black is the SM.

Fig. 12 suggests that prospects here might be better than for h giving a signal in the range $122 < m_h < 128$ GeV. Indeed, there are solutions with $R_{\tau\tau H}^{Exclusion} = 0.5$ that would need about 20fb^{-1} to be uncovered.

Observability of the other Higgses shows, in many cases, very good prospects, gain in the $\bar{\tau}\tau$ channels, $R_{\tau\tau h}^{Exclusion} > 0.6$ are obtained, see fig. 13. Therefore it is worth pursuing searches of h , for $m_h < 120$ GeV in the $\bar{\tau}\tau$ channel. A^0 could also be uncovered with the same luminosity, in fact fig. 13 shows the correlation between h and A^0 in the $\bar{\tau}\tau$ channel. There, of course, remains also many situations with $R_{\tau\tau}^{Exclusion} < 0.2$ that would be difficult to decipher.

4.2 Model B: a light stop with large mixing in the stop sector

We now turn to the maximal mixing case and restrict ourselves to $m_{\tilde{t}_2} = 600$ GeV ($m_{\tilde{t}_1} = 200$ GeV). Compared to the previous case without mixing one notes that there is a reduction in $R_{\tau\tau H}$. This is mainly driven by the drop in $gg \rightarrow H$, see fig. 14, very low values are also due to quite small $h\tau\bar{\tau}$ couplings.

The most noticeable change is the correlation between R_{ZZ} and $R_{\gamma\gamma+2 \text{ jets}}$, see fig. 15. We now easily find $R_{\gamma\gamma+2 \text{ jets}} > R_{ZZ}$. The spread in this correlation has increased. One can find scenarios with $R_{ZZ} < 1$ even for $R_{\gamma\gamma} > 2$. For $R_{\gamma\gamma} \sim 2$, $R_{\gamma\gamma+2 \text{ jets}} > 2$ is attained.

The visibility of A^0 and h is little affected by the stop mixing. Our conclusions are little changed. Again it is very important to pursue the search in the $\bar{\tau}\tau$ channel.

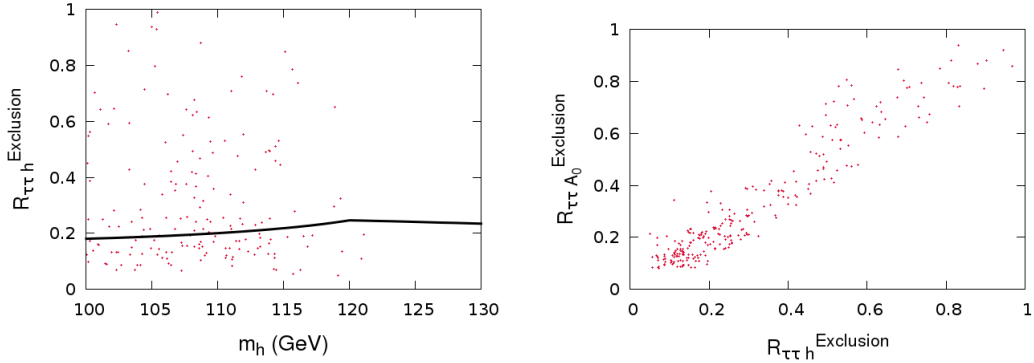


Figure 13: $R_{\tau\tau h}^{exclusion}$ as a function of m_h for $122 < m_H < 128$ GeV in the case where A^0 and h are not degenerate within 10 GeV (left panel). The right panel shows the correlations between the h and A^0 in the τ channels. No mixing in the stop sector is applied. The line in black in the left panel represents the SM.

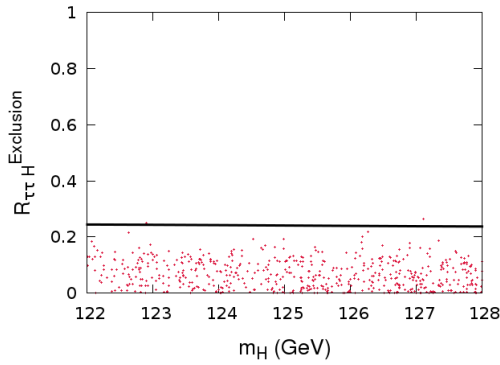


Figure 14: $R_{\tau\tau H}$ in the same mass $122 < m_H < 128$ GeV in the case of maximal stop mixing and $m_{\tilde{t}_2} = 600$ GeV. The line in black is the SM.

5 Conclusion

Despite the fact that no sign of supersymmetry has been found so far, the BMSSM framework is a very efficient set up that extends the realm of the MSSM in a most natural way as concerns the realisation of the Higgs. In the MSSM framework there is some tension with naturalness for a Higgs mass of 125 GeV that requires heavy stops, in the BMSSM this is not an issue. Although one must exercise extreme care with the so called tantalising hints for a Higgs signal around this mass, 125 GeV, it is extremely important to scrutinise the properties of the Higgs with such a mass in many models, in particular the BMSSM which represents an effective implementation of a variety of supersymmetric models having the same field content as the MSSM. The tantalising hints have come also with the temptation, even if premature, of reading from the results of ATLAS and CMS, despite the uncertainty of the measurements, that the signals in the inclusive

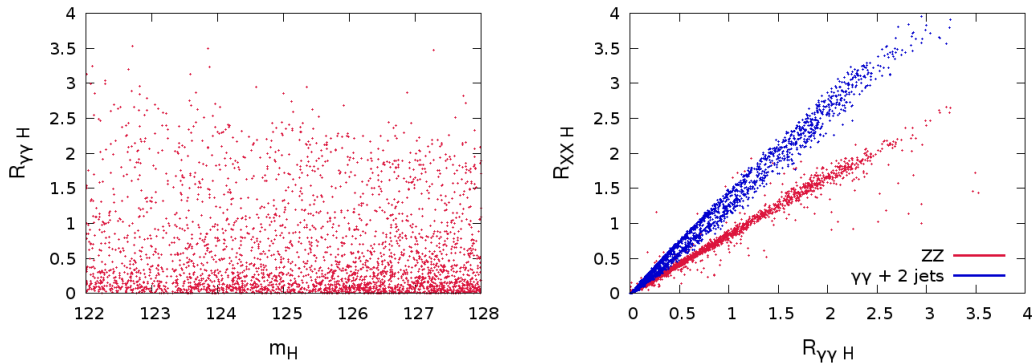


Figure 15: We show here the allowed region in the plane $m_H, R_{\gamma\gamma}$ (left panel) and the associated correlations between $R_{\gamma\gamma}, R_{ZZ}$ and $R_{\gamma\gamma+2\text{jets}}$ for $122 < m_H < 128$ GeV (right panel) with maximal mixing and $m_{\tilde{t}_2} = 600$ GeV.

2γ channel, the $2\gamma + \text{jets}$ and perhaps in the $ZZ \rightarrow 4l$ to be higher than what is expected from the SM. Such scenarios are practically impossible to attain in the MSSM, a possibility that has been entertained would make the naturalness argument even more excruciating. It is therefore very important to find out whether some configurations, especially those leading to enhancements in these most important channels can be realised in the BMSSM. As important is to find out how these enhancements or signals are correlated and how different kinds of correlations can be realised. We have shown that a vanilla BMSSM where stops are at very moderate masses and with little mixing easily allows enhancements in all these channels for $m_h \sim 125$ GeV with the constraint that the rate $ZZ \rightarrow 4l$ would generally be higher than the rate $\gamma\gamma + 2\text{jets}$. A light stop with large mixings in the stop sector offers more possibilities especially as concerns correlations between these three important channels. Our study also reveals that although it is easier to have such realisations work for the lightest Higgs of the BMSSM, solutions where it is the heaviest Higgs that has a mass around 125 GeV also exist. Once a signal at 125 GeV has been confirmed a better measurement of the rates, in particular the 2γ (inclusive and exclusive) as well as the $4l$ would narrow considerably the parameter space of the BMSSM. At the same time as more precision is achieved and more luminosity is gathered one can constrain the models through the other Higgses (those outside the 125 GeV window) but also through other channels of the Higgs at 125 GeV. Our study reveals that in both cases it is crucially important and telling to investigate the $\bar{\tau}\tau$ channel. We have not folded in the possible constraints from flavour physics and dark matter as we have argued that this introduces some model dependencies (including those from cosmology) but it is clear now that we have entered a fascinating era. The study we have conducted is an example which shows that even before any new direct signal of New Physics is discovered, the study of the Higgs, once confirmed, will give important clues on the New Physics. We eagerly await more data and analyses from the experiments and we urge, once more, our colleagues to provide as much information as possible on the data so that one can gain access to the different individual subchannels that make up an inclusive channel.

A Addendum: Tevatron and the $\bar{b}b$ channel

While this work was being finalised, the Tevatron Collaborations released new analyses[43] pointing out to a possible signal in $VH \rightarrow V\bar{b}b$ channel with a rate that could be compatible with the Standard Model expectation and with a mass that could correspond to where the excesses are seen at the LHC. This would seem at first sight to disfavour a scenario where $g_{h\bar{b}b}$ is very much reduced. However, one must keep in mind that since the decay $H \rightarrow \bar{b}b$ dominates for $m_h = 125$ GeV, a suppression of the coupling by a factor two does not imply a suppression of the branching ratio by a factor two. The suppression is much more modest and there can still be a significant enhancement of the diphoton channel without suppressing too much the $VH \rightarrow V\bar{b}b$ channel. It must be stressed that a more precise measurement of the latter process would really be helpful. Indeed, there exists also a correlation between the diphoton (inclusive) channel and this channel, as shown in fig 16.

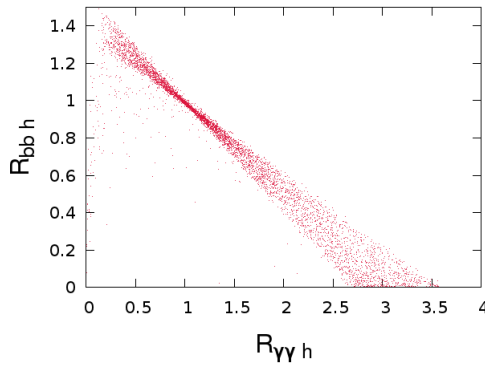


Figure 16: *Correlation between diphoton channel ($R_{\gamma\gamma}$) and the $VH \rightarrow V\bar{b}b$ ($R_{\bar{b}b}$) in the non-mixing scenario.*

References

- [1] ATLAS Collaboration, (2012), arXiv:1202.1408 [hep-ex].
- [2] CMS Collaboration, (2012), arXiv:1202.1488 [hep-ex].
- [3] S. Heinemeyer, O. Stal, and G. Weiglein, (2011), arXiv:1112.3026 [hep-ph].
- [4] A. Arbey, M. Battaglia, A. Djouadi, F. Mahmoudi, and J. Quevillon, Phys.Lett. **B708**, 162 (2012), arXiv:1112.3028 [hep-ph].
- [5] M. Carena, S. Gori, N. R. Shah, and C. E. Wagner, (2011), arXiv:1112.3336 [hep-ph].
- [6] P. Draper, P. Meade, M. Reece, and D. Shih, (2011), arXiv:1112.3068 [hep-ph].
- [7] J. Cao, Z. Heng, J. M. Yang, Y. Zhang, and J. Zhu, (2012), arXiv:1202.5821 [hep-ph].
- [8] J. L. Feng, K. T. Matchev, and D. Sanford, (2011), arXiv:1112.3021.
- [9] L. Aparicio, D. Cerdeno, and L. Ibanez, (2012), arXiv:1202.0822 [hep-ph].

- [10] N. Desai, B. Mukhopadhyaya, and S. Niyogi, (2012), arXiv:1202.5190 [hep-ph].
- [11] L. J. Hall, D. Pinner, and J. T. Ruderman, (2011), arXiv:1112.2703 [hep-ph].
- [12] A. Arvanitaki and G. Villadoro, (2011), arXiv:1112.4835 [hep-ph].
- [13] U. Ellwanger, (2011), arXiv:1112.3548.
- [14] J. F. Gunion, Y. Jiang, and S. Kraml, (2012), arXiv:1201.0982 [hep-ph].
- [15] S. King, M. Muhlleitner, and R. Nevzorov, (2012), arXiv:1201.2671 [hep-ph].
- [16] Z. Kang, J. Li, and T. Li, (2012), arXiv:1201.5305 [hep-ph].
- [17] D. Carmi, A. Falkowski, E. Kuflik, and T. Volansky, (2012), arXiv:1202.3144 [hep-ph].
- [18] A. Azatov, R. Contino, and J. Galloway, (2012), arXiv:1202.3415 [hep-ph].
- [19] J. Espinosa, C. Grojean, M. Muhlleitner, and M. Trott, (2012), arXiv:1202.3697 [hep-ph].
- [20] A. Brignole, J. A. Casas, J. R. Espinosa, and I. Navarro, Nucl. Phys. **B666**, 105 (2003), hep-ph/0301121.
- [21] M. Dine, N. Seiberg, and S. Thomas, Phys. Rev. **D76**, 095004 (2007), arXiv:0707.0005 [hep-ph].
- [22] I. Antoniadis, E. Dudas, and D. Ghilencea, JHEP **0803**, 045 (2008), arXiv:0708.0383 [hep-ph].
- [23] I. Antoniadis, E. Dudas, D. Ghilencea, and P. Tziveloglou, Nucl.Phys. **B808**, 155 (2009), arXiv:0806.3778 [hep-ph].
- [24] P. Batra and E. Ponton, Phys.Rev. **D79**, 035001 (2009), arXiv:0809.3453 [hep-ph].
- [25] C. Petersson and A. Romagnoni, (2011), arXiv:1111.3368 [hep-ph].
- [26] J. Casas, J. Espinosa, and I. Hidalgo, JHEP **0401**, 008 (2004), hep-ph/0310137.
- [27] S. Cassel, D. Ghilencea, and G. Ross, Nucl.Phys. **B825**, 203 (2010), arXiv:0903.1115 [hep-ph].
- [28] M. Carena, K. Kong, E. Ponton, and J. Zurita, Phys.Rev. **D81**, 015001 (2010), arXiv:0909.5434 [hep-ph].
- [29] I. Antoniadis, E. Dudas, D. Ghilencea, and P. Tziveloglou, Nucl.Phys. **B831**, 133 (2010), arXiv:0910.1100 [hep-ph].
- [30] M. Carena, E. Ponton, and J. Zurita, Phys.Rev. **D82**, 055025 (2010), arXiv:1005.4887 [hep-ph].
- [31] I. Antoniadis, E. Dudas, D. Ghilencea, and P. Tziveloglou, Nucl.Phys. **B848**, 1 (2011), arXiv:1012.5310 [hep-ph].
- [32] M. Carena, E. Ponton, and J. Zurita, (2011), arXiv:1111.2049 [hep-ph].
- [33] F. Boudjema and G. Drieu La Rochelle, Phys.Rev. **D85**, 035011 (2012), arXiv:1112.1434 [hep-ph].

- [34] D. Piriz and J. Wudka, Phys.Rev. **D56**, 4170 (1997), hep-ph/9707314.
- [35] ATLAS & CMS Collaborations, *ATLAS-CONF-2011-157,CMS-PAS-HIG-11-023*, <http://cdsweb.cern.ch/record/1399607/files/HIG-11-023-pas.pdf>.
- [36] S. Kraml *et al.*, (2012), 1203.2489.
- [37] CMS Collaboration, S. Chatrchyan *et al.*, (2012), arXiv:1202.3478 [hep-ex].
- [38] LHC Higgs Cross Section Working Group, S. Dittmaier *et al.*, (2011), 1101.0593.
- [39] ATLAS Collaboration, (2012), arXiv:1202.1414 [hep-ex].
- [40] CMS Collaboration, *CMS-PAS-HIG-11-030*, <http://cdsweb.cern.ch/record/1406346/files/HIG-11-030-pas.pdf>.
- [41] A. Djouadi, Phys.Lett. **B435**, 101 (1998), hep-ph/9806315.
- [42] G. Belanger, F. Boudjema, and K. Sridhar, Nucl.Phys. **B568**, 3 (2000), hep-ph/9904348.
- [43] TEVNPH (Tevatron New Phenomena and Higgs Working Group), CDF and D0 Collaboration, (2012), 1203.3774, Preliminary results prepared for the Winter 2012 Conferences.